2014 IEEE International Conference on Robotics & Automation (ICRA)
Hong Kong Convention and Exhibition Center
May 31 - June 7, 2014. Hong Kong, China

Time Delay Sliding Mode Control of Nonholonomic Wheeled Mobile Robot: Experimental Validation

Spandan Roy, Sambhunath Nandy, *Member, IEEE*, Ranjit Ray, *Member, IEEE* and Sankar Nath Shome, *Member, IEEE*

***Abstract*— In this endeavor, a hybrid control strategy has been proposed for composite path tracking control of a nonholonomic wheeled mobile robotic (WMR) system under parametric and nonparametric uncertainties. A WMR, often in practical circumstances, undergoes through various parametric changes. Moreover, modeling of WMR in presence of friction, slip or skid, backlash etc. is very difficult. These factors, which make the system model more cumbersome, are normally ignored but their effects are compensated through appropriate control methods. Conventional Sliding Mode Control (SMC) is such a method but it is susceptible to chattering due to high switching gains and reasonable tracking accuracy is sacrificed to avoid chattering. On the other hand, Time Delay Control (TDC) technique is highly efficient to assure robustness against unknown dynamics but it is unable to eliminate approximation errors that arise due to introduced delay. Considering the aforesaid difficulties of SM and TD controllers a hybrid control methodology christened as Time Delay Sliding Mode Control (SMC-TD) is adopted in this work for accurate path tracking of nonholonomic WMR. The SMC-TD is absolutely a judicious blending of SMC and TDC strategies aiming at elimination of the individual shortcomings while retaining the positive advantages. Detail features and advantages of the proposed controller are presented in greater length along with the experimental results, which are very promising.**

I. INTRODUCTION

Nonholonomic systems are defined, in general, as systems that satisfy certain non-integrable constraints. Such constraints may arise as a result of physical kinematic constraints imposed on the system which are expressed in terms of the generalized velocities of the system and cannot be integrated over time, and thus cannot be expressed in terms of the generalized coordinates only. Nonholonomic mobile robots have received a lot of attention in the past two decades because of their ability to work through large application domains, such as: (i) transportation, (ii) planetary exploration, (iii) surveillance, (iv) security, (v) military targets tracking, and (vi) human-machine-interfaces for people with mobility deficiency. Design of suitable controllers for Path tracking of WMR with appropriate trajectory commands are well addressed by the research communities and controllers are implemented mainly based on kinematic and dynamic model. Amongst the kinematic model based controllers, De wit and Khennouf [1] designed a piecewise continuous closed loop controller based on the kinematic model of the robot and showed exponential stabilization around the origin. Guldner and Utkin [2] applied SMC using Lyapunov's function. Jiang and Pomet [3] used back stepping technique for adaptive control of nonholonomic systems with unknown parameters. Hamel and Meizel [4] claimed robustness against localization errors in their proposed controller. Aguilar et al. [5] proposed a SMC based control approach for path-following of a car-like robot while ensuring robustness against localization and curvature errors. A SM based controller for posture stabilization and trajectory tracking of a WMR was reported by Chawa [6].

Relevant assumptions during kinematic modeling are responsible for modeling errors, which create difficulties in efficient control of WMR. These circumstances necessitate consideration of the dynamic model of WMR (Kolmanovsky and McClamroch [7], Fierro and Lewis [8]). Gradually, many researchers followed the dynamic model based controller design approach. Yang and Kim [9] adopted SMC for simple trajectory tracking of WMR in polar coordinates for posture representation using computed-torque technique. Corradini and Orlando [10] used discrete time SMC for trajectory tracking control. Chen et al. [11] reported an adaptive SMC method where adaptive control is used to approximate the upper bounds of uncertainty. To tackle higher bound of uncertainty SMC suffers from chattering effect due to increase in switching gains, which may also activate high frequency un-modeled dynamics causing harmful effect on robotic systems. Furthermore, nominal model of the system is required for bound estimation, which is tough to achieve for a complex WMR system. Oriolo et al. [12] compared the performance of dynamic feedback linearization against the simple linear feedback linearization as well as nonlinear feedback linearization for trajectory tracking and posture stabilization. Sun [13] used exact feedback linearization and pole placement approach to devise a trajectory tracking controller. Feedback linearization technique for path tracking of a WMR incorporating the actuator dynamics was reported by Nandy et al. [14]. Shojaei et al. [15] reported an inverse dynamics and robust-PID based trajectory tracking control strategy. Realization of feedback linearization control through inverse dynamics formulation requires exact knowledge of the hardware parameters. While performing various tasks different payload sensors are used which in turn affect the dynamic parameters like mass, moment of inertia (MOI), centre of mass (COM), wheel radius etc. Lizarralde et al. [16] applied Kalman Filter (KF) in association with the

Spandan Roy is engaged as Scientist Trainee at Robotics and Automation Lab., CSIR-Central Mechanical Engineering Research Institute, Durgapur, India (phone: +918981467353; e-mail: sroy002@gmail.com).

Sambhunath Nandy is engaged as Principal Scientist at Robotics and Automation Lab., CSIR-Central Mechanical Engineering Research Institute, Durgapur, India (e-mail: snandy@cmeri.res.in).

Ranjit Ray is engaged as Senior Scientist at Robotics and Automation Lab., CSIR-Central Mechanical Engineering Research Institute, Durgapur, India (e-mail: ranjitray@cmeri.res.in).

Sankar Nath Shome is engaged as Chief Scientist and Head of Robotics and Automation Lab., CSIR-Central Mechanical Engineering Research Institute, Durgapur, India (e-mail: shomecmeri@gmail.com).

model predictive control technique to estimate the states of WMR accurately. Wang and Wilson [17] used KF for estimating the orientation and position of WMR. A KF based active observer entailing robust path following control of WMR was addressed by Coelho and Nunes [18].

Presented here a time-delay sliding mode control (SMC-TD) methodology for accurate path tracking of WMR, inspired from Morioka et al. [19]. This hybrid control methodology takes care the parametric uncertainties caused due to variation in hardware parameters and also evaluates the Lagrange multipliers including combined effect of the un-modeled dynamic components such as friction slip, skid etc. through estimate of an appropriate function, using the TDC [20] method. This control algorithm also helps to negate the estimation error using the switching logic. The performance of the controller has been verified through extensive simulation and experimentation utilizing a WMR, named 'Drishti' designed and developed by the Robotics and Automation Laboratory of CSIR-CMERI, Durgapur, India.

The article is organized as follows: The dynamics of WMR is briefly described in section 2. Section 3 describes the proposed hybrid control methodology in detail. Section 4 and section 5 presents the simulation study and experimental results while Section 6 concludes the entire work.

II. DYNAMICS OF WMR

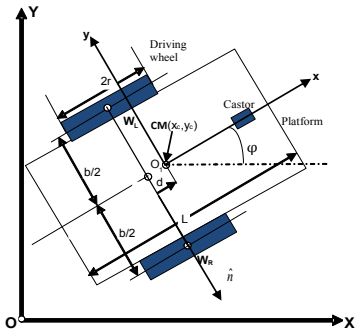

Figure 1. Schematic diagram of the wheeled mobile robot

A WMR is considered as an appropriate example of a nonholonomic system. A two wheeled vehicle shown in Fig. 1 is analyzed in detail by Nandy et al. [14]. The vehicle is driven by two motors connected to the two wheels of radius *r* which are separated by distance *b*. Length of the vehicle is considered as *L*. A body-fixed (moving) coordinate system is placed at the COM, which is assumed to be at an offset distance *d* along *x*-axes from the axle of the robot. Let, m_{P} be the mass of the mobile robot platform without the driving wheels, the motors rotor, and gearbox rotor, m_w represents the mass of each driving wheel and the associated motor rotor including gearbox rotor, I_{P} be the MOI of the platform about a vertical axes passing through the COM of the platform, I_{w} is the equivalent wheel MOI referred to wheel axis, Δ is the offset between COM of the overall system and the platform and I_m represents MOI of each wheel and associated motor including gearbox rotor about a wheel diameter passing through the z-axis. The position of the WMR can be specified by three generalized coordinates x_c, y_c, φ where, (x_c, y_c) are the coordinates of the COM of the system. To specify coordinates of any point on the wheels two more variables θ_r and θ_l (i.e. rotation of the right and left wheels respectively, so long as the axes of the wheels are fixed with respect to the cart) are needed. So, the generalized coordinate vector of the system contains five generalized coordinates $(i.e.\ n=5)$ and is expressed as $\mathbf{q} \in \Re^5 = (x_c, y_c, \varphi, \theta_r, \theta_l)^T$.

The Lagrange-Euler based equation of motion has been derived in [14]. The dynamic equations are presented as,

$$m\ddot{x}_c + K(\ddot{\varphi}\sin\varphi + \dot{\varphi}^2\cos\varphi) - \lambda_1\sin\varphi - \cos\varphi(\lambda_2+\lambda_3) = 0, \quad (1)$$

$$m\ddot{y}_c - K(\ddot{\varphi}\cos\varphi - \dot{\varphi}^2\sin\varphi) + \lambda_1\cos\varphi - \sin\varphi(\lambda_2+\lambda_3) = 0, \quad (2)$$

$$I\ddot{\varphi} + K(\ddot{x}_c\sin\varphi - \ddot{y}_c\cos\varphi) - d\lambda_1 + \tfrac{b}{2}(\lambda_3-\lambda_2) = 0, \quad (3)$$

$$I_w\ddot{\theta}_r + \lambda_2 r = \tau_r, \quad (4)$$

$$I_w\ddot{\theta}_l + \lambda_3 r = \tau_l. \quad (5)$$

The values of m, K and I are selected according to [14]. The constraints (rolling without slipping) of WMR are:

$$\dot{y}_c\cos\varphi - \dot{x}_c\sin\varphi - \dot{\varphi}d = 0, \quad (6)$$

$$\dot{x}_c\cos\varphi + \dot{y}_c\sin\varphi + \tfrac{b}{2}\dot{\varphi} - r\dot{\theta}_r = 0, \quad (7)$$

$$\dot{x}_c\cos\varphi + \dot{y}_c\sin\varphi - \tfrac{b}{2}\dot{\varphi} - r\dot{\theta}_l = 0. \quad (8)$$

Equations (1-5) is written compactly in the form leading to,

$$\mathbf{M}(\mathbf{q})\ddot{\mathbf{q}} + \mathbf{V}(\mathbf{q},\dot{\mathbf{q}}) = \mathbf{B}\boldsymbol{\tau} - \mathbf{A}^T(\mathbf{q})\boldsymbol{\lambda}, \quad (9)$$

where,

$$\mathbf{M}(\mathbf{q}) = \begin{bmatrix} m & 0 & K\sin\varphi & 0 & 0 \\ 0 & m & -K\cos\varphi & 0 & 0 \\ K\sin\varphi & -K\cos\varphi & I & 0 & 0 \\ 0 & 0 & 0 & I_w & 0 \\ 0 & 0 & 0 & 0 & I_w \end{bmatrix},$$

$$\mathbf{V}(\mathbf{q},\dot{\mathbf{q}}) = \begin{bmatrix} K\dot{\varphi}^2\cos\varphi \\ K\dot{\varphi}^2\sin\varphi \\ 0 \\ 0 \\ 0 \end{bmatrix}, \quad \mathbf{B}(\mathbf{q}) = \begin{bmatrix} 0 & 0 \\ 0 & 0 \\ 0 & 0 \\ 1 & 0 \\ 0 & 1 \end{bmatrix}, \quad \boldsymbol{\tau} = \begin{bmatrix} \tau_r \\ \tau_l \end{bmatrix},$$

$$\mathbf{A}(\mathbf{q}) = \begin{bmatrix} -\sin\varphi & \cos\varphi & -d & 0 & 0 \\ -\cos\varphi & \sin\varphi & -\frac{b}{2} & r & 0 \\ -\cos\varphi & -\sin\varphi & \frac{b}{2} & 0 & r \end{bmatrix}, \quad \boldsymbol{\lambda} = \begin{bmatrix} \lambda_1 \\ \lambda_2 \\ \lambda_3 \end{bmatrix}.$$

Here, $\mathbf{q} = [x_c \ y_c \ \varphi \ \theta_r \ \theta_l] \in R^{5\times1}$ is the vector of generalized coordinates, $\boldsymbol{\tau} = [\tau_r \ \tau_l] \in R^{2\times1}$ is the vector of generalized forces, $\mathbf{M} \in R^{5\times5}$ is the inertia matrix, $\mathbf{V} \in R^{5\times1}$ is the matrix that contains Coriolis, centripetal and gravitational terms, $\mathbf{B} \in R^{5\times2}$ represent the control input matrix, $\mathbf{A} \in R^{3\times5}$ and $\boldsymbol{\lambda} \in R^{3\times1}$ are the constraint matrix and vector of constraint forces (Lagrange multipliers), respectively. The value of vector $\boldsymbol{\lambda}$ is found solving (1), (2), (3) and utilizing (6-8) as,

$$\lambda_1 = \left(Kr - mrd\right)\left(\ddot{\theta}_r - \ddot{\theta}_l\right)/b + mr^2\left(\dot{\theta}_l^2 - \dot{\theta}_r^2\right)/2b, \quad (10)$$

$$\lambda_2 = \left[\Omega_1 + \ddot{\varphi}\left(I - Kd\right) + Kb\dot{\varphi}^2\right]/b, \quad (11)$$

$$\lambda_3 = \left[\Omega_2 + \ddot{\varphi}\left(Kd - I\right) + Kb\dot{\varphi}^2\right]/b, \quad (12)$$

where,

$$\Omega_1 = mbr(\ddot{\theta}_r + \ddot{\theta}_l)/2 + (rmd^2 - rKd)(\ddot{\theta}_r - \ddot{\theta}_l)/2b - mbd\dot{\varphi}^2 + r^2\left(\dot{\theta}_r^2 - \dot{\theta}_l^2\right)(md - K)/4b,$$

$$\Omega_2 = mbr(\ddot{\theta}_r + \ddot{\theta}_l)/4 + (rmd^2 - rKd)(\ddot{\theta}_l - \ddot{\theta}_r)/b - m\tfrac{b}{2}d\dot{\varphi}^2 - r^2\left(\dot{\theta}_r^2 - \dot{\theta}_l^2\right)(md - K)/2b.$$

Subtracting (8) from (7) yields,

$$\dot{\varphi} = r\left(\dot{\theta}_r - \dot{\theta}_l\right)/b. \tag{13}$$

Substituting (10), (11) and (12) into (1-3) and using (13) as well as (4-5) the new dynamics in compact form is written as,

$$\bar{\mathbf{M}}(\mathbf{q})\ddot{\mathbf{q}} + \bar{\mathbf{V}}(\mathbf{q},\dot{\mathbf{q}}) = \mathbf{u}, \tag{14}$$

where,

$$\bar{\mathbf{M}}(\mathbf{q}) = \begin{bmatrix} m & 0 & K\sin\varphi & k_1 & k_2 \\ 0 & m & -K\cos\varphi & k_3 & k_4 \\ K\sin\varphi & -K\cos\varphi & I & -k_5 & k_5 \\ k_1 & k_3 & -k_5 & I_w & 0 \\ k_2 & k_4 & k_5 & 0 & I_w \end{bmatrix},$$

$$k_1 = \left((mdr - Kr)/b\sin\varphi - mr/2\cos\varphi\right),$$

$$k_2 = \left((Kr - mdr)/b\sin\varphi - mr/2\cos\varphi\right),$$

$$k_3 = \left((Kr - mdr)/b\cos\varphi - mr/2\sin\varphi\right),$$

$$k_4 = \left((mdr - Kr)/b\cos\varphi - mr/2\sin\varphi\right), k_5 = r\left(I - Kd\right)/b,$$

$$\bar{\mathbf{V}}(\mathbf{q},\dot{\mathbf{q}}) = \begin{bmatrix} md\dot{\varphi}^2\cos\varphi + mr^2\sin\varphi\left(\dot{\theta}_r^2 - \dot{\theta}_l^2\right)/2b \\ md\dot{\varphi}^2\sin\varphi - mr^2\cos\varphi\left(\dot{\theta}_r^2 - \dot{\theta}_l^2\right)/2b \\ Kr^2\left(\dot{\theta}_r^2 - \dot{\theta}_l^2\right)/2b \\ -Kr\dot{\varphi}^2/2 \\ -Kr\dot{\varphi}^2/2 \end{bmatrix}, \ \mathbf{u} = \mathbf{B}\boldsymbol{\tau}.$$

Equation (14) is rewritten as

$$\ddot{\mathbf{q}} = \mathbf{f}(\mathbf{q},\dot{\mathbf{q}}) + \boldsymbol{\beta}(\mathbf{q})\mathbf{u}, \tag{15}$$

where, $\mathbf{f}(\mathbf{q},\dot{\mathbf{q}}) = -\bar{\mathbf{M}}^{-1}(\mathbf{q})\bar{\mathbf{V}}(\mathbf{q},\dot{\mathbf{q}})$, $\boldsymbol{\beta}(\mathbf{q}) = \bar{\mathbf{M}}^{-1}(\mathbf{q})$.

III. Controller Design

A. Conventional Sliding Mode Control (SMC) Approach

SMC is a special category of Variable Structure Control, whose structures are switched judiciously according to certain switching logic to achieve desired system behavior. SMC provides robustness against any parametric uncertainties and other disturbances, which must lie in the image space of the input i.e. matched uncertainties [21] as well as within the capacity of the actuators in real situation. The design of SM controller is carried out in two steps: design of appropriate sliding surface (s = 0) and making the surface attractive by an appropriate control law so that the system trajectory points towards the sliding surface.

In general, if a system with n degrees of freedom (DOF) to be controlled and for each DOF if the order turns out to be N, the sliding surface for each state variable is selected constructing a function of the error and its derivatives as follows,

$$s_i = \left(\tfrac{d}{dt} + \Lambda_i\right)^{N-1} e_i, \text{ for } i = 1,2,\ldots,n, \tag{16}$$

where, e_i's are the state errors and $\Lambda_i > 0$ represent the i^{th} state gains pertaining to the state error convergence rate towards the equilibrium points. The finite reaching condition and assured decrement of distance along all system trajectories to the sliding surface is established by choosing the overall control law $\mathbf{u}$ such that outside of surface for each DOF the following condition is fulfilled:

$$\tfrac{1}{2}\tfrac{d}{dt}s_i^2 \le -\eta_i|s_i| \quad \text{for } i = 1,2,\ldots,n,$$
$$\Rightarrow \dot{s}_i s_i \le -\eta_i|s_i|, \tag{17}$$

where, $\eta_i > 0$ for $i = 1,2,\ldots,n$ is satisfied. The term η_i is responsible for finite time reaching condition. By adapting the condition mentioned in (17), the time t_{si} to reach $s_i = 0$ satisfies the following criterion [22]:

$$t_{si} \le |s_i(0)|/\eta_i.$$

If the sliding surface is reached at $t = t_{si}$ and ideal sliding motion takes place, then the switching function satisfies $s_i = 0$ for all $t > t_{si}$. This condition implies that $\dot{s}_i = 0$ for all $t \ge t_{si}$ when system lies on the sliding surface. Higher choice of η_i for a given $|s_i(0)|$ would ensure faster reaching phase with increase of switching gain which might induce the possibility of chattering simultaneously. Perturbing the system dynamics given in (15) accordingly to,

$$\Delta\mathbf{f} = \mathbf{f} - \hat{\mathbf{f}}, \tag{18}$$

$$\boldsymbol{\beta} = (\mathbf{I} + \boldsymbol{\Gamma})\hat{\boldsymbol{\beta}}, \tag{19}$$

where, $\hat{\boldsymbol{\beta}}$ and $\hat{\mathbf{f}}$ are the nominal values of the terms $\boldsymbol{\beta}$ and $\mathbf{f}$, respectively. $\boldsymbol{\Gamma}\hat{\boldsymbol{\beta}}$ is the perturbation in $\hat{\boldsymbol{\beta}}$ where $\boldsymbol{\Gamma}$ represents a $n \times n$ matrix that maps uncertainties with respect to $\hat{\boldsymbol{\beta}}$. The sliding surface considering all DOF (each represents a 2nd order system) of WMR is chosen (as hyper plane) and written compactly as,

$$\mathbf{s} = \dot{\mathbf{e}} + \boldsymbol{\Lambda}\mathbf{e}, \tag{20}$$

where, $\mathbf{e}$ and $\dot{\mathbf{e}}$ are the position and velocity tracking errors respectively. The position and velocity errors are given by:

$$\mathbf{e}(t) = \mathbf{q}(t) - \mathbf{q}^d(t), \ \dot{\mathbf{e}}(t) = \dot{\mathbf{q}}(t) - \dot{\mathbf{q}}^d(t),$$

where, $\mathbf{q}^d(t)$ is the desired trajectory to be tracked by the robot. The hyper plane in (20) represents individual lines with slope $-\Lambda_i$ corresponds to each DOF along which the trajectory slides. Differentiating (20) with respect to time,

$$\dot{\mathbf{s}} = \ddot{\mathbf{e}} + \boldsymbol{\Lambda}\dot{\mathbf{e}} = \ddot{\mathbf{q}} - \ddot{\mathbf{q}}^d + \boldsymbol{\Lambda}\dot{\mathbf{e}} = \mathbf{f} + \boldsymbol{\beta}\mathbf{u} - \ddot{\mathbf{q}}^d + \boldsymbol{\Lambda}\dot{\mathbf{e}}. \tag{21}$$

Now, the choice of the composite control input $\mathbf{u} = \hat{\boldsymbol{\beta}}^{-1}(\ddot{\mathbf{q}}^d - \hat{\mathbf{f}} - \boldsymbol{\Lambda}\dot{\mathbf{e}})$ does not lead to $\dot{\mathbf{s}} = \mathbf{0}$ (dynamics while in sliding mode) as $\hat{\boldsymbol{\beta}} \ne \boldsymbol{\beta}$ and $\hat{\mathbf{f}} \ne \mathbf{f}$ due to the presence of the various forms of uncertainties and errors. To provide robustness against these errors the control law is devised as:

$$\mathbf{u} = \hat{\mathbf{u}} - \mathbf{G}\mathbf{sgn}(\mathbf{s}), \tag{22}$$

where, $\hat{\mathbf{u}} = \hat{\boldsymbol{\beta}}^{-1}(\ddot{\mathbf{q}}^d - \hat{\mathbf{f}} - \boldsymbol{\Lambda}\dot{\mathbf{e}})$ is the best estimate of the equivalent control input for the system. The discontinuous switching term represented by $\mathbf{G}\mathbf{sgn}(\mathbf{s})$ across the surface ($\mathbf{s}$ = $\mathbf{0}$) provides the necessary input to satisfy the sliding

condition (17) despite presence of uncertainties on the governing model of the system. The switching gain vector $\mathbf{G}$ is evaluated from (17) as per following sequences:

$$\dot{\mathbf{s}}\mathbf{s} \le -\boldsymbol{\eta}|\mathbf{s}|$$
$$\Rightarrow \left[\mathbf{f}+\boldsymbol{\beta}\mathbf{u}-\ddot{\mathbf{q}}^d+\boldsymbol{\Lambda}\dot{\mathbf{e}}\right]\mathbf{s} \le -\boldsymbol{\eta}|\mathbf{s}|$$
$$\Rightarrow \left[\mathbf{f}+\boldsymbol{\beta}\hat{\boldsymbol{\beta}}^{-1}(\ddot{\mathbf{q}}^d-\hat{\mathbf{f}}-\boldsymbol{\Lambda}\dot{\mathbf{e}})-\boldsymbol{\beta}\mathbf{G}\mathbf{sgn}(\mathbf{s})-\ddot{\mathbf{q}}^d+\boldsymbol{\Lambda}\dot{\mathbf{e}}\right]\mathbf{s} \le -\boldsymbol{\eta}|\mathbf{s}|$$
$$\Rightarrow \boldsymbol{\beta}\mathbf{G} \ge \boldsymbol{\eta}+\left[\mathbf{f}-\hat{\mathbf{f}}-(\boldsymbol{\beta}\hat{\boldsymbol{\beta}}^{-1}-\mathbf{I})\hat{\mathbf{f}}+(\boldsymbol{\beta}\hat{\boldsymbol{\beta}}^{-1}-\mathbf{I})(\ddot{\mathbf{q}}^d-\boldsymbol{\Lambda}\dot{\mathbf{e}})\right]\mathbf{sgn}(\mathbf{s})$$
$$\Rightarrow \boldsymbol{\beta}\mathbf{G} \ge \boldsymbol{\eta}+\left[\Delta\mathbf{f}+\boldsymbol{\Gamma}(\ddot{\mathbf{q}}^d-\hat{\mathbf{f}}-\boldsymbol{\Lambda}\dot{\mathbf{e}})\right]\mathbf{sgn}(\mathbf{s})$$
$$\Rightarrow \mathbf{G} \ge \boldsymbol{\beta}^{-1}\left[\boldsymbol{\eta}+\mathbf{F}+\mathbf{D}\boldsymbol{\Phi}\right], \quad (23)$$

where, the uncertainty terms $\mathbf{F}$, $\mathbf{D}$, and $\boldsymbol{\Phi}$ are defined as,

$$\left|\hat{f}_i-f_i\right|=|\Delta f_i| \le F_i,\ \left|\Gamma_{ij}\right| \le D_{ij},\ \left|\ddot{q}_i^d+\hat{f}_i+\Lambda_i\dot{e}_i\right| \le \Phi_i.$$

The aforesaid computations are well defined for $|\mathbf{s}| \neq \mathbf{0}$. To remove the discontinuity in the control law introduced in (22) a reasonably small positive error boundary ε is incorporated in the control law as follows,

$$\mathbf{u}=\hat{\mathbf{u}}-\mathbf{G}\mathbf{sat}(\mathbf{s}/\varepsilon). \quad (24)$$

Next, the hybrid strategy for better performance is presented.

B. Sliding Mode Control with Time Delay (SMC-TD)

To make the SM controller to work in a broader range higher uncertainty bounds may be considered. This in turn requires higher switching gains, which leads to chattering. To avoid chattering we need to increase ε in lieu of tracking accuracy. In practical scenario backlash, friction, slip or skid etc. normally exist but not considered for modeling due to extensive modeling effort and complicated nature of the model, which necessitates the incorporation of TDC. The SMC-TD approach provides two major advantages; (i) reduction in switching gains through approximation of the un-modeled dynamics and other combined disturbances and (ii) elimination of approximation error that arises from time delay logic of TDC.

The dynamics presented in (9) is rewritten in modified form as,

$$\hat{\mathbf{M}}(\mathbf{q})\ddot{\mathbf{q}}+\mathbf{H}_1(\mathbf{q},\dot{\mathbf{q}},\ddot{\mathbf{q}},\boldsymbol{\lambda})=\mathbf{u}, \quad (25)$$

where, $\mathbf{H}_1(\mathbf{q},\dot{\mathbf{q}},\ddot{\mathbf{q}},\boldsymbol{\lambda})=(\mathbf{M}(\mathbf{q})-\hat{\mathbf{M}}(\mathbf{q}))\ddot{\mathbf{q}}+\mathbf{V}(\mathbf{q},\dot{\mathbf{q}})+\mathbf{A}^T(\mathbf{q})\boldsymbol{\lambda}$. $\mathbf{H}_1$ can be thought to contain friction, slip or skid and other un-modeled dynamics terms. $\hat{\mathbf{M}}$ represents the nominal value of $\mathbf{M}$ and the perturbation in $\mathbf{M}$ can be written as,

$$\Delta\mathbf{M}=\mathbf{M}-\hat{\mathbf{M}}. \quad (26)$$

$\Delta\mathbf{M}$ is assumed to represent a symmetric positive definite matrix. Incorporation of TDC needs the following to be fulfilled [20],

$$\left\|\mathbf{I}-\mathbf{M}^{-1}(\mathbf{q})\hat{\mathbf{M}}(\mathbf{q})\right\|<1, \text{ for all } \mathbf{q} \in \Re^{5\times 1} \quad (27)$$

For controller design convenience (25) is modified as,

$$\ddot{\mathbf{q}}=\boldsymbol{\xi}+\hat{\mathbf{g}}\mathbf{u}, \quad (28)$$

where, $\boldsymbol{\xi}=-\hat{\mathbf{M}}^{-1}\mathbf{H}_1$ and $\hat{\mathbf{g}}=\hat{\mathbf{M}}^{-1}$. To compare the performance of the two controllers the sliding surface has been kept same as in (20). Differentiating (20) yields:

$$\dot{\mathbf{s}}=\ddot{\mathbf{e}}+\boldsymbol{\Lambda}\dot{\mathbf{e}}=\ddot{\mathbf{q}}^d-\ddot{\mathbf{q}}+\boldsymbol{\Lambda}\dot{\mathbf{e}}=\ddot{\mathbf{q}}^d-\boldsymbol{\xi}-\hat{\mathbf{g}}\mathbf{u}+\boldsymbol{\Lambda}\dot{\mathbf{e}}. \quad (29)$$

To achieve $\dot{\mathbf{s}}=\mathbf{0}$ the best approximation is chosen as,

$$\hat{\mathbf{u}}(t)=\hat{\mathbf{g}}^{-1}(t)(\ddot{\mathbf{q}}^d(t)-\boldsymbol{\xi}(t)+\boldsymbol{\Lambda}\dot{\mathbf{e}}(t)). \quad (30)$$

Considering delay time (t_d) equal to sampling time and assuming t_d to be reasonably small we can approximate the following using time delay logic utilizing (28) as,

$$\boldsymbol{\xi}(t) \cong \boldsymbol{\xi}(t-t_d)=\ddot{\mathbf{q}}(t-t_d)-\hat{\mathbf{g}}(t-t_d)\mathbf{u}(t-t_d). \quad (31)$$

Infinite sampling frequency can ideally establish (31). But, an approximation error will always be embedded and it is assumed to be bounded by,

$$\|\boldsymbol{\xi}(t)-\boldsymbol{\xi}(t-t_d)\| \le \delta. \quad (32)$$

Finally, the control law is selected as follows,

$$\mathbf{u}(t)=\hat{\mathbf{u}}(t)+\hat{\mathbf{g}}^{-1}(t)\boldsymbol{\psi}\mathbf{sgn}(\mathbf{s}/\varepsilon)=\hat{\mathbf{g}}^{-1}(t)(\hat{\mathbf{g}}(t-t_d)\mathbf{u}(t-t_d)+\ddot{\mathbf{q}}^d(t)-\ddot{\mathbf{q}}(t-t_d)+\boldsymbol{\Lambda}\dot{\mathbf{e}}(t)+\boldsymbol{\psi}\mathbf{sgn}(\mathbf{s}/\varepsilon)), \quad (33)$$

here, $\boldsymbol{\psi}$ is a fixed gain column vector unlike a time varying gain of conventional SMC.

C. Stability Analysis

Considering the Lyapunov function candidate as,

$$V(\mathbf{E},t)=\tfrac{1}{2}\mathbf{s}^2, \quad (34)$$

where, $\mathbf{E}=[\mathbf{e}\ \ \dot{\mathbf{e}}]^T$. Differentiation of (34) yields,

$$\dot{V}(\mathbf{E},t)=\tfrac{1}{2}\tfrac{d}{dt}\mathbf{s}^2=(\ddot{\mathbf{e}}(t)+\boldsymbol{\Lambda}\dot{\mathbf{e}})\mathbf{s}=(\ddot{\mathbf{q}}^d-\ddot{\mathbf{q}}+\boldsymbol{\Lambda}\dot{\mathbf{e}})\mathbf{s},$$
$$\Rightarrow\ \dot{V}(\mathbf{E},t)=(\ddot{\mathbf{q}}^d(t)-\boldsymbol{\xi}(t)-\hat{\mathbf{g}}\mathbf{u}(t)+\boldsymbol{\Lambda}\dot{\mathbf{e}}(t))\mathbf{s}. \quad (35)$$

Substituting (31) and (33) into (35) yields,

$$\dot{V}(\mathbf{E},t)=-(\boldsymbol{\xi}(t)-\boldsymbol{\xi}(t-t_d))\mathbf{s}-\boldsymbol{\psi}|\mathbf{s}| \le \delta|\mathbf{s}|-\boldsymbol{\psi}|\mathbf{s}| \le -\boldsymbol{\gamma}|\mathbf{s}|, \quad (36)$$

with $\boldsymbol{\psi} \ge \delta+\boldsymbol{\gamma}$ and $|\mathbf{s}|=\{|s_1|,|s_2|,\cdots,|s_5|\}$.

Finally, the SMC-TD control law takes the form,

$$\mathbf{u}(t)=\hat{\mathbf{u}}(t)+\hat{\mathbf{g}}^{-1}(t)\boldsymbol{\psi}\mathbf{sat}(\mathbf{s}/\varepsilon)=\hat{\mathbf{g}}^{-1}(t)(\hat{\mathbf{g}}(t-t_d)\mathbf{u}(t-t_d)+\ddot{\mathbf{q}}^d(t)-\ddot{\mathbf{q}}(t-t_d)+\boldsymbol{\Lambda}\dot{\mathbf{e}}(t)+\boldsymbol{\psi}\mathbf{sat}(\mathbf{s}/\varepsilon)). \quad (37)$$

IV. SIMULATION RESULTS

Based on the above formulation circular and lawn mower reference paths are selected for simulation. Unlike SMC, SMC-TD does not require the knowledge of the Coriolis, centripetal, Lagrange multipliers and other un-modeled factors. Thus, (25) is used for the SMC-TD, whereas SM controller requires (14). The controller parameters are chosen as $\text{diag}(\boldsymbol{\Lambda})=\{2,2,2,2,2\}$, $t_d=0.1$s for both the controllers. To verify the performance of the controllers the system is subjected to a sinusoid (absolute value) payload variation [23] as depicted in Fig. 2 taking WMR nominal mass 35 kg.

A. Circular Path Tracking

The trajectory definition for circular path with radius R = 1.5 m and angular velocity $\dot{\varphi}^d=0.25$ rad/s is given as,

$$x_c^d=R\cos(\dot{\varphi}^d t+\varphi_0),\ y_c^d=R+R\sin(\dot{\varphi}^d t+\varphi_0),$$
$$\varphi^d=\varphi_0+\dot{\varphi}^d t, \theta_R^d=\dot{\varphi}^d\left(R+b/2\right)/r, \theta_L^d=\dot{\varphi}^d\left(R-b/2\right)/r.$$

The initial position vector is chosen as $[x_{c0},\ y_{c0},\ \varphi_0]=\left[1.5\ 1.5\ 0\right]^T$. Fig. 3 depicts the desired circular path to be tracked and Fig. 4 and Fig. 5

demonstrates the superior tracking performance of SMC-TD over SMC in terms of x_c and y_c position error.

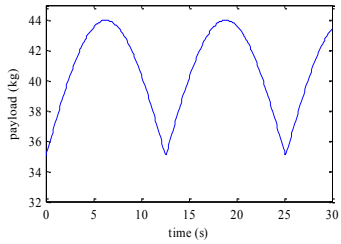

Figure 2. Sinusoid (absolute value) payload

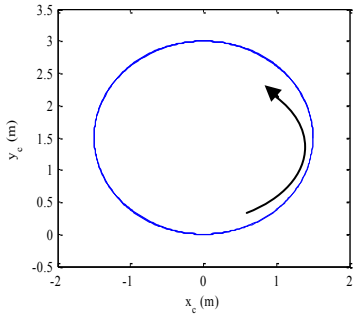

Figure 3. Desired circular trajectory

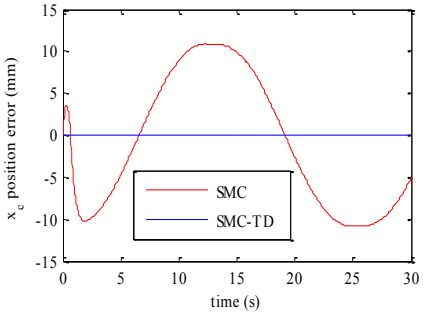

Figure 4. x_c position error comparison

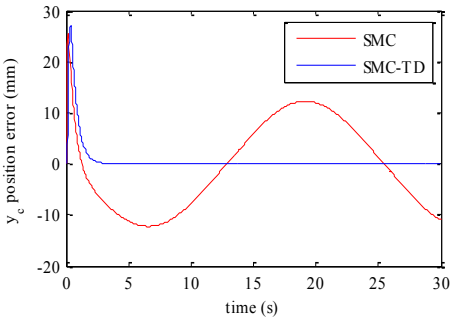

Figure 5. y_c position error comparison

B. Lawn Mower Path Tracking

The next path selected for study is a lawn mower path [24]. Lawn mower path, represented in Fig. 6, is very useful for survey purposes. The trajectory definitions are given as:

$$x_c^d = 0.1t + 0.3\sin(0.4t),\ y_c^d = 1.2 + 1.2\cos(0.2t - T).$$

The wheel velocities are chosen to be square wave of same magnitude and the left wheel velocity is half of the time period delayed from the right wheel (Fig. 7). As a perfect square signal is discontinuous in nature, they are approximated applying Fourier series as follows,

$$w(t) = \tfrac{(a+c)}{2} + 2\tfrac{(a-c)}{\pi}\sum_{n=1,3,}^{\infty}\left(\sin\tfrac{n\pi}{2}\cos\tfrac{2n\pi}{T}t\right)/n,$$

where, a = 3 and c = 1.6 signifies the maximum and minimum wheel velocity, T = 25s is the time period of the signal. Trajectories for other generalized coordinates are chosen as:

$$\varphi^d = c\int\left(\dot\theta_R - \dot\theta_L\right)dt,\ \theta_R^d = \int\dot\theta_R dt,\ \theta_L^d = \int\dot\theta_L dt.$$

The initial condition is taken as $\mathbf{q}_0^d = [0\ 0\ 0\ 0\ 0]^T$.

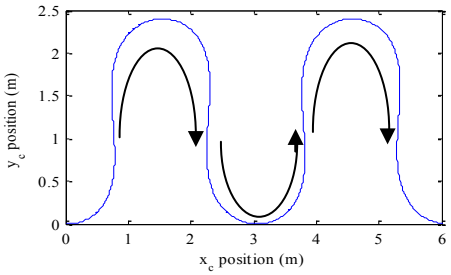

Figure 6. Desired lawn mower path

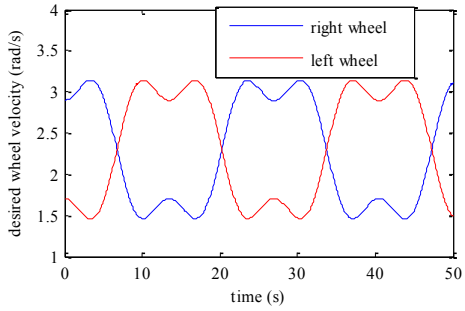

Figure 7. Desired wheel velocities to achieve lawn mower path

Fig. 8 demonstrates the relative performance comparison of the two controllers under the similar sinusoidal payload variation in terms of path error. Path error is defined as the Euclidean error distance. Significantly improved performance of SMC-TD over SM controller is observed.

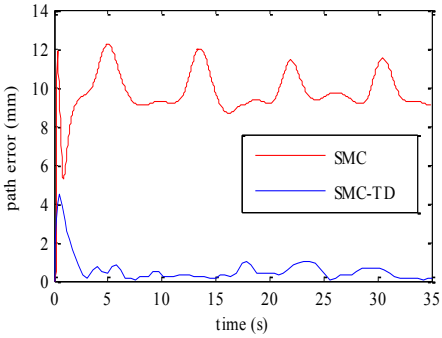

Figure 8. Path error comparison for lawn mower path

V. Experimental Results

Performance of the proposed controller is verified with several experiments with Drishti (Fig. 9), a two-wheel differentially driven robotic platform designed and developed

at Robotics and Automation group of CSIR-CMERI. The solid wheels with radius of 96 mm are stiff enough that point contact with the ground can be assumed and are mounted on an axle of 414 mm long. A small passive caster wheel with 70 mm diameter is placed in the rear of the vehicle at a distance of 374 mm from the axle. The chassis of the robot contains a single board computer (SBC, PC-104+ architecture, Pentium M 1.8 GHz), two Maxon motors (90W each), transmission elements, electronics, and three set 24 V, 22Ah high energy density Li-polymer batteries and the sensor suite. Each motor is equipped with an incremental encoder and a gearbox with reduction ratio 91. The communication between the server and client of Drishti is maintained through a 'D-link' USB modem. Experimentally, it is not exactly possible to imitate a sinusoidal payload variation like simulation study. Here, the robot carries a 6 kg Laser Range Finder as extra payload. To create a time varying payload and to achieve various COM and variations of inertia, further 3 kg load was added/removed alternatively on/from the WMR platform at random places as shown in Fig. 10.

Figure 9. WMR-Dristhi

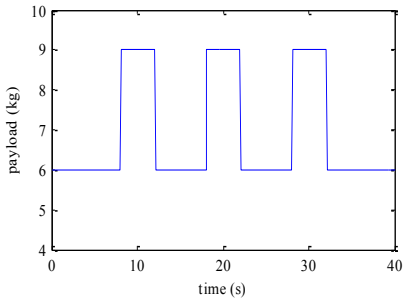

Figure 10. Payload variation for experimentation

A. Circular Path

The circular path tracked by the WMR, when two different controllers are employed, is demonstrated in Fig. 11. The corresponding absolute x_c and y_c positional errors are plotted in Fig. 12 and Fig. 13 respectively. From the received sensor data it is observed that positional information at some instants remain same giving spikes in the error plots of SMC. This gives an indication of slippage. As slip is not considered while modeling, performance of SMC degrades. But due to its robustness property it still tries to overcome that and pushes the error downwards periodically. SMC-TD is capable of managing such un-modeled dynamics using the time delay logic and gives the superior performance. Again, with the switching logic it eliminates the approximation error to a great extent. The performances of the two controllers are depicted in Table-I by means of the average error (Avg. err.) for long term performance and evaluating the maximum error (Max. err.) for momentary performance. The percentage errors are calculated with respect to diameter of circular path.

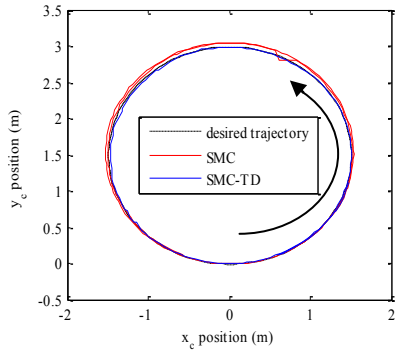

Figure 11. Circular path tracking comparison

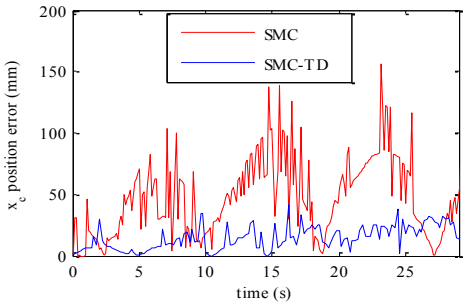

Figure 12. x_c position error comparison

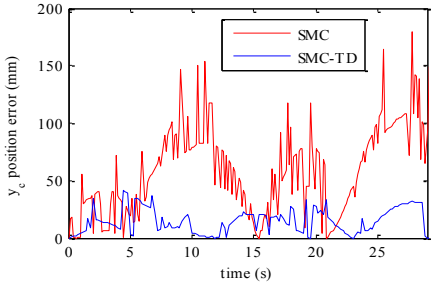

Figure 13. y_c position error comparison

TABLE I. PERFORMANCE COMPARISON FOR CIRCULAR PATH

Controllers	x_c Position Error (mm)				y_c Position Error (mm)			
	Avg. err.	*% Avg. err.*	*Max. err.*	*% Max. err.*	*Avg. err.*	*% Avg. err.*	*Max . err.*	*% Max err.*
SMC	49.4	1.65	156	5.2	59.3	1.98	179	5.97
SMC-TD	14.8	0.49	41	1.37	14.6	0.49	41	1.37

B. Lawn Mower Path

The lawn mower path tracked by WMR with SMC and SMC-TD is shown in Fig. 14 with an initial position $[x_{c0}, y_{c0}, \varphi_0] = [0\ 0\ 0]^T$. Fig. 15 presents the path errors incurred by the different controllers. The path tracking accuracy of SMC-TD is better than SMC for both the loops.

Table-II provides a comparative study where the percentage errors are calculated with respect to maximum path length.

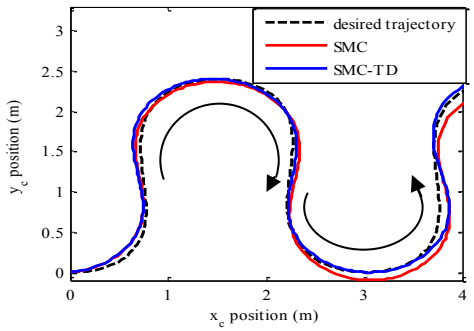

Figure 14. Lawn mower path tracking comparison

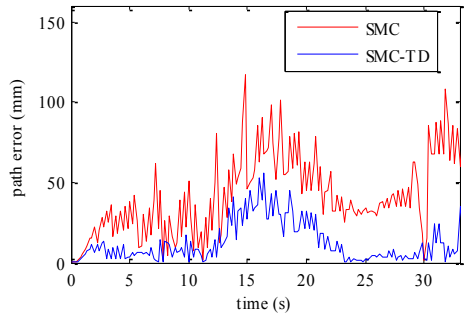

Figure 15. Path error for lawn mower path

TABLE II. PERFORMANCE COMPARISON FOR LAWN MOWER PATH

Controllers	Path Error (mm)			
	Avg. err.	*% Avg. err.*	*Max. err.*	*% Max err.*
SMC	42.62	1.74	116.89	4.76
SMC-TD	12.52	0.51	55.66	2.27

VI. CONCLUSION

This paper proposed a time delay sliding mode based hybrid control strategy and validated through simulation and experimentation for efficient path tracking of WMR. The proposed hybrid controller (SMC-TD) judiciously fuses the best features of the SM and TDC, providing assured robustness to the system from two fronts, overcoming their individual shortcomings. The SMC-TD aims at the reduction of the switching gain of the SMC as well as ensures reduced modeling effort of the complex WMR through the embedded TD logic. On the other front, SMC deals with the approximation error generated from TDC applying the switching logic. The experiments show promising result in terms of the path tracking performance of the SMC-TD with WMR compared to the conventional SM controller.

REFERENCES

[1] C. C. de Wit and H. Khennouf, "Quasi continuous stabilizing controllers for nonholonomic systems: Design and robustness consideration," in *Proc. Eur. Control. Conf.*, Rome, Italy, pp. 2207–2212, 1995.

[2] J. Guldner and V. I. Utkin, "Stabilization of nonholonomic mobile robots using Lyapunov functions for navigation and sliding mode control," *In Proc. IEEE Conf. Decis. Control,*. Lake Buena Vista, FL, pp. 2967-2972, Dec. 1994.

[3] Z. P. Jiang and J. -B. Pomet, "Combining backstepping and time-varying techniques for a new set of adaptive controllers," *In Proc. IEEE Conf. Decis. Control.*, Lake Buena Vista, FL, pp. 2207-2212, Dec. 1994.

[4] T. Hamel and D. Meizel, "Robust control laws for wheeled mobile robots," *Int. J. Syst. Sci.*, vol. 27,no. 8, pp. 695-704, 1996.

[5] L. E. Aguilar, T. Hamel and P. Soueres, "Robust path following control for wheeled robots via sliding mode techniques," in *Proc. IEEE/RSJ Int. Conf. Intell. Rob. Syst.*, vol. 3, pp. 1389-1395, Sep. 1997.

[6] D. Chawa, "Sliding mode tracking control of wheeled mobile robots in polar coordinates," *IEEE Trans. Control. Syst. Technol.*, Vol. 12, No. 4, pp. 637-644, July 2004.

[7] I. Kolmanovosky and N. H. McClamroch, "Developments in nonholonomic control problems," *IEEE Control. Syst. Mag.*, pp. 20-36, Dec. 1995.

[8] R. Fierro and F. L. Lewis, "Robust practical point stabilization of a nonholonomic mobile robot using neural networks*," J. Intell. Robotic Syst.*, Vol. 20, pp. 295-317, 1997.

[9] J. -M. Yang and J.-H. Kim, "Sliding mode control for trajectory tracking of nonholonomic wheeled mobile robots," *IEEE Trans. Robot. Autom.*, vol. 15, pp. 578-587, Jun. 1999.

[10] M. L. Corradini and G. Orlando, "Control of mobile robots with uncertainties in the dynamical model: a discrete time sliding mode approach with experimental results," *Control. Eng. Prac.*, vol. 10, pp. 23-34, 2002.

[11] C. Chen, T. S. Li, Y. Yeh and C. Chang, "Design and implementation of an adaptive sliding-mode dynamic controller for wheeled mobile robots," *Mechatron*., vol. 19, pp. 156-166, 2009.

[12] G. Oriolo, A. De Luca and M. Vendittelli, "WMR control via dynamic feedback linearization: design, implementation, and experimental validation," *IEEE Trans. Control. Syst. Technol.*, vol. 10, no. 6, pp. 835–852, 2002.

[13] S. Sun, "Designing approach on trajectory-tracking control of mobile robot," *Robot. Comput.-Integr. Manuf.*, vol. 21, pp. 81-85, 2005.

[14] S. Nandy, G. Chakraborty, C. S. Kumar and S. N. Shome, "A modular approach to detail dynamic formulation and control of wheeled mobile robot," in p*roc. IEEE Int. Conf. Mechatron. Autom.*, pp. 1471-1478, 2011.

[15] K. Shojaei, A. M. Shahari and B. Tabibian, "Design and implementation of an inverse dynamics controller for uncertain nonholonomic robotic systems," *J. Intell. Robotic Syst.*, vol. 71, pp. 65-83, 2013.

[16] F. Lizarralde, E. Nunes, , L. Hsu, and J. Wen, "Mobile robot navigation using sensor fusion," in *Proc. IEEE Int. Conf. Robot. Autom.*, pp. 458-463, 2003.

[17] J. Wang and W. Wilson, "3D relative position and orientation estimation using Kalman filter for robot control," in *Proc. IEEE Int. Conf. Robot. Autom.*, pp. 2638–2645, 1992.

[18] P. Coelho and U. Nunes, "Path-following control of mobile robots in presence of uncertainties," *IEEE Trans. Robot. Autom.*, vol. 21, no. 2, pp. 252-261, April, 2005.

[19] H. Morioka, A. Sabanovic, A. Uchibori, K. Wada and M. Oka, "Application of time-delay-control in variable structure motion control systems," in *proc. IEEE Int. Symp. Ind. Electron.*, vol. 2, pp. 1313-1318, 2001.

[20] T. C. Hsia and L. S. Gao, "Robot manipulator control using decentralized linear time-invariant time-delayed joint controllers", in *Proc. IEEE Int. Conf. Robot. Autom*., vol. 3, pp. 2070-2075, 1990.

[21] G. Leitmann, "On the efficiency of nonlinear control in uncertain linear systems," *ASME J. Dyn. Syst. Meas. Control.*, vol. 103, pp. 95-102, 1981.

[22] C. Edwards and S. K. Spurgeon. *Sliding mode control: theory and applications.* Taylor and Francis, 1998.

[23] S. Roy, S. N. Shome, S. Nandy, R. Ray and V. Kumar, "Trajectory following control of AUV: a robust approach," *J. Inst. Eng. India Ser. C,* vol. 94, no. 3, pp. 253–265, 2013.

[24] S. Roy, S. Nandy, S. N. Shome and R. Ray, "Robust position control of an autonomous underwater vehicle: a comparative study," in *proc. IEEE Int. Conf. Autom. Sci. Eng.*, pp. 1002-1007, 2013.